

(1971).

²P. W. Anderson, B. I. Halperin, and C. M. Varma, *Philos. Mag.* **25**, 1 (1972).

³W. A. Phillips, *J. Low Temp. Phys.* **7**, 351 (1972).

⁴For a recent review, see S. Hunklinger and W. Arnold, in *Physical Acoustics*, edited by W. P. Mason (Academic, New York, 1976), Vol. XII, p. 155; see also J. E. Graebner and B. Golding, *Bull. Am. Phys. Soc.* **24**, 493 (1979).

⁵W. M. Goubau and R. H. Tait, *Phys. Rev. Lett.* **34**, 1220 (1975).

⁶J. L. Black, *Phys. Rev. B* **17**, 2740 (1978).

⁷R. B. Kummer, R. C. Dynes, and V. Narayanamurti, *Phys. Rev. Lett.* **40**, 1187 (1978).

⁸J. C. Lasjaunias, A. Ravex, M. Vandorpe, and S. Hunklinger, *Solid State Commun.* **17**, 1045 (1975).

⁹R. B. Stephens, *Phys. Rev. B* **8**, 2896 (1973). See Fig. 1 of this paper.

¹⁰J. P. Harrison, G. Lombardo, and P. P. Peressini, *J. Phys. Chem. Solids* **29**, 557 (1968).

¹¹M. P. Zaitlin and A. C. Anderson, *Phys. Rev. B* **12**, 4475 (1975).

¹²W. H. Haemmerle, B. Golding, and F. S. L. Hsu, *Bull. Am. Phys. Soc.* **25**, 195 (1980); see also D. P. Jones, N. Thomas, and W. A. Phillips, *Phil. Mag. B* **38**, 271 (1978).

¹³M. T. Lopenon, R. C. Dynes, and V. Narayanamurti, to be published.

Monte Carlo Simulation of Eu³⁺-Doped BeF₂ Glass

S. A. Brawer and M. J. Weber

Lawrence Livermore Laboratory, University of California, Livermore, California 94550

(Received 4 March 1980)

Monte Carlo simulations of the structure of Eu³⁺-doped BeF₂ glass show that in contrast to the almost perfect fourfold coordination of Be by F, the rare-earth sites are disordered and no fixed coordination number can be defined. The calculated distribution of Eu³⁺ electronic energy levels is in general agreement with the inhomogeneous broadening observed in optical spectra and measured using laser-induced fluorescence line-narrowing techniques.

PACS numbers: 61.40.Df, 61.20.Ja, 78.50.Ec

Optical and magnetic resonance spectra of paramagnetic ions in glass are characterized by large inhomogeneous broadening attributed to site-to-site variations in the local structure of the impurity sites.¹ There have been numerous attempts to infer the local glass structure from the optical spectra of the impurity,¹ but these have been frustrated by the lack of uniqueness of any such construction. In this paper we take a new approach to the problem of the optical spectra of impurities in glass, with specific application to BeF₂:Eu³⁺. To investigate the disorder and distribution of local environments at activator ion sites in inorganic glasses, we have (1) simulated a rare-earth-doped BeF₂ glass by the Monte Carlo (MC) technique of statistical mechanics, (2) used laser-induced fluorescence line narrowing (FLN) techniques to measure site-dependent energy level splittings, and (3) compared measured optical spectra with energy level distributions predicted from the simulated structure. The results are in good agreement with experiment and show very clearly the variations in local structure and fields. This approach can be extended to calculate

spectroscopic properties of many paramagnetic ions in glass.

Our model glass system consisted of 199 ions: 65 Be²⁺, 133 F⁻, and 1 Eu³⁺ in a cubic cell of side 13.82 Å (the density of 2.06 g/cm³ corresponding to the doping concentration of 1.3 mol% EuF₃). Because of its simple energy level structure, Eu³⁺ provides a convenient probe of the local fields.² The interionic potential energy included a Coulomb term and a Born-Mayer repulsion for ions *i* and *j* of the form $A_{ij} \exp(-\sigma r)$. The Coulomb potential was evaluated as the Ewald sum by use of the Hansen approximation.³ The A_{ij} for Be-F ions was the same as used by Woodcock, Angell, and Cheeseman.⁴ For Eu-F ions it was chosen to make the first peak in the Eu-F radial distribution function (RDF) occur at 2.35 Å, the sum of the Pauling radii⁵; for Eu-Be ions it was set equal to zero. $\sigma = 3.448 \text{ \AA}^{-1}$ for all ions.

Computations were made with an array processor (Floating Point Systems Model 120 B) and a PDP-11/55 host computer: this combination generated 250 000 configurations per hour. A high-

temperature fluid was simulated first by making a run of 16 million steps (individual ion displacements) at a temperature of 1667 K where sufficient diffusion occurs to ensure complete randomization of the fluid. Glasses were formed by starting with one of the high-temperature fluid configurations and carrying out the MC process while slowly lowering the temperature. During the cooling process the step size was adjusted to keep the acceptance rate between 40% and 50%; a total of 200 000 steps were made. At the final temperature (900 K) no diffusion occurred. Every 100 000th configuration of the initial high-temperature fluid was quenched in this way. Because the model system contained only 1 rare earth (RE), 159 different initial fluid configurations were quenched. The collection of these low-temperature configurations is the glass. Other details of the simulation are the same as described elsewhere.⁶

The glass structure for ions more than 4 Å from the RE was similar to that of simple amorphous BeF₂ and consisted of a nearly continuous random network of distorted BeF₄ tetrahedra joined at vertices with fluctuating Be-F-Be angles. A few defects in the form of coordination irregularities were observed, as discussed in Ref. 6. Calculated RDF's are in good agreement with experimental data for BeF₂.^{7,8} Our MC results are the same as those obtained in molecular dynamics simulations of BeF₂.^{4,9}

Our particular interest is the structure near the RE. The Eu-F and Eu-Be RDF's, which give the number of ions per unit volume at dis-

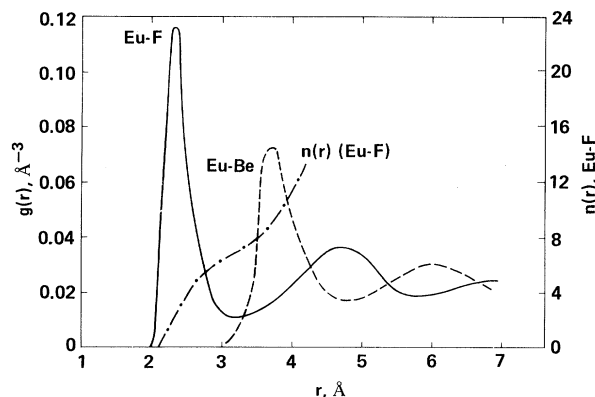


FIG. 1. Calculated Eu-F and Eu-Be radial distribution functions g_- and g_+ , respectively, for computer-simulated BeF₂:Eu³⁺ glass. (The vertical scale for g_+ is half the left-hand scale.) The quantity n is the average coordination of Eu by F.

tance r , are shown in Fig. 1. The distributions of Eu-F and Eu-Be distances are broad. Some F ions are as close as 2.1 Å; there are no Be ions closer than 3.0 Å. Included in Fig. 1 is $n(r)$, the average coordination number of the RE by F, obtained by integrating the RDF out to r . As shown in Table I, the site-to-site variations in coordination number are large. In addition, we find that the closer a F is to the RE, the greater the probability that it is nonbridging, i.e., bonded to only one Be. (If a Be-F separation is ≤ 2.4 Å, we call them "bonded".) Thus for F ions at distances of 2.4, 2.6, 2.8, 3.0, and 4.0 Å (± 0.1 Å) from the RE, the probabilities of being nonbridging are 0.80, 0.55, 0.32, 0.08, and 0.02, respectively. This statistical distribution of bridging and nonbridging fluorines about the RE is a type of disorder not measured by the conventional RDF. Since all F have at least one Be neighbor within 2.4 Å, there are no free F ions.

The presence of the RE introduces another kind of short-range order into the glass. We find that the BeF₄ tetrahedra adjacent to the RE are oriented so that one vertex points toward the RE. Specifically, consider a Be bonded to a F which is within a distance r of the RE (the distance r is the cutoff for the RE first coordination shell and is to some extent arbitrary). Let p be the probability that all the other F ions bonded to that particular Be are farther than r from the RE and hence are not ligands. Thus p is the probability that the BeF₄ tetrahedron is monodentate for ligands within distance r of the RE. For $r = 2.25, 2.5, 2.75,$ and 3.0 Å, the computed p values are 1.0, 0.99, 0.93, and 0.87, respectively. Therefore the smaller r is, the more probable that BeF₄ tetrahedra adjacent to the RE are monodentate.

In summary, the RE is complexed mainly, but not entirely, by nonbridging F, with no local symmetry and with site-to-site fluctuations in coordination number and RE-F distances. Each disordered coordination polyhedron shares mostly

TABLE I. Fraction of Eu³⁺ ions with exactly n first-neighbor fluorine ions within a sphere of radius r , based on a computer-simulated BeF₂:Eu³⁺ glass.

Radius r (Å)	First-neighbor coordination number n				
	5	6	7	8	9
2.7	0.09	0.29	0.47	0.15	0
3.0	0	0.12	0.34	0.48	0.06

corners with adjacent BeF_4 tetrahedra in agreement with Pauling's second rule for ionic structures.⁵ This rule is obeyed statistically; the smaller the cutoff defining the first coordination sphere, the fewer the number of exceptions.

To test the validity of our simulations of the local structure at the RE site, we calculated the electronic energy levels of Eu^{3+} using a point-charge model of the crystal field (CF). While such a calculation is only of qualitative significance, it offers further insight into the structure at the RE sites. To limit the number of parameters, we restrict ourselves to the 7F_0 and 7F_1 manifolds of Eu^{3+} for which the second-order CF terms are of overwhelming importance. The point-charge CF is given by

$$V = -A \sum_L \frac{q_L}{R_L^3} \sum_{q=-2}^2 Y_q^2(\theta_L, \varphi_L) U_q^2, \quad (1)$$

where ligand L of charge q_L is at distance R_L from the RE, Y_q^2 is a second-order spherical harmonic, U_q^2 is the reduced tensor operator for the f electrons of Eu^{3+} , and A is a positive free parameter. To clarify the relation between energy and structure, only F ligands within 2.75 \AA of the RE are assumed to contribute to the CF.¹⁰ The energy levels of the 7F_0 and 7F_1 manifolds of Eu^{3+} for 159 configurations of the glass were computed from Eq. (1) by diagonalizing the 16×16 matrix in the basis of the $J=0, 1, 2, 3$ manifolds of the 7F term. The constant A and the centers of gravity of the manifolds were chosen to give the best fit to the observed spectra.

Both broadband- and laser-excited fluorescence spectra from the 5D_0 state to levels of 7F were recorded and compared with the calculated energy levels. The BeF_2 sample contained 0.5 wt% EuF_3 and was measured at $\approx 30 \text{ K}$. The two upper curves in Fig. 2 are the experimental fluorescence spectra for broadband excitation into levels above 5D_0 . The histograms are the calculated distribution of Eu^{3+} energy levels for 159 sites. (The energy of the 5D_0 level was taken to be constant.) Although the site dependence of the transition probabilities is unknown at present, the asymmetry of the ${}^5D_0 \rightarrow {}^7F_0$ profile and the magnitude of the inhomogeneous broadening of the ${}^5D_0 \rightarrow {}^7F_1$ band are both successfully modeled.

The Stark splitting of subsets of sites were probed with use of a tunable flashlamp-pumped Rhodamine-6G dye laser (Chromatix CMX-4) and fluorescence line narrowing techniques.² Excitation was via the weak ${}^7F_0 \rightarrow {}^5D_0$ transition¹¹ and photon counting detection was necessary. To

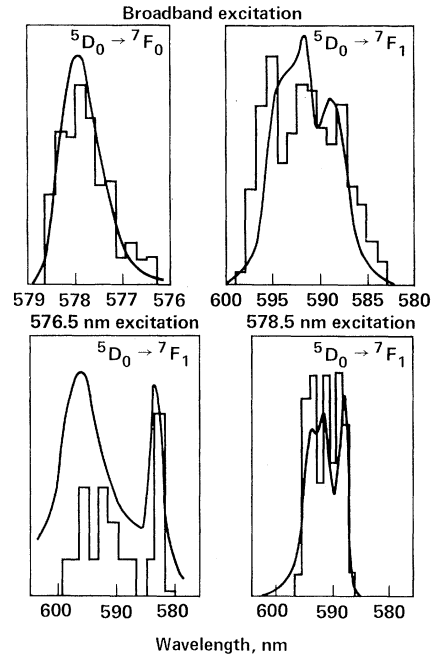


FIG. 2. Measured fluorescence spectra (smooth curves) and calculated energy-level distributions (histograms) for Eu^{3+} in BeF_2 glass. Energy levels were calculated using a point-charge model of the crystal field. The two top curves are broadband-excited spectra; the two bottom curves are narrow-band laser-excited spectra.

avoid distortion to spectral diffusion by ion-ion cross relaxation, the fluorescence was monitored during the first $500 \mu\text{s}$ of the $\approx 10\text{-ms}$ decay. The two lower curves in Fig. 2 show the emission observed for excitation on the short- and long-wavelength sides of the 7F_0 - 5D_0 band. The histograms are calculated distributions of 7F_1 energies for those sites having 7F_0 - 5D_0 energies within $\pm 0.2 \text{ nm}$ of the excitation wavelength. The histograms again model the overall splitting and distribution of the 7F_1 energy levels for different sites. The smallest and the largest 7F_1 splitting observed experimentally differed by a factor of ≈ 4 ; the calculated energy levels show a similar range of relative splittings.

To correlate energy levels with structure at each RE site, we do a principal axis transformation. The matrix $M_{ij} = \sum_L r_i(L)r_j(L)/R_L^5$, where r_1, r_2, r_3 are the x, y, z components of the position of ligand L , is diagonalized by a simple rotation of the coordinate system. If $R_i(L)$ are the ligand positions with respect to the new principal axes, the eigenvalues of M are $\lambda_i = \sum_L R_i^2(L)/R_L^5$. We assume $\lambda_1 > \lambda_2 > \lambda_3$. To examine the variation of

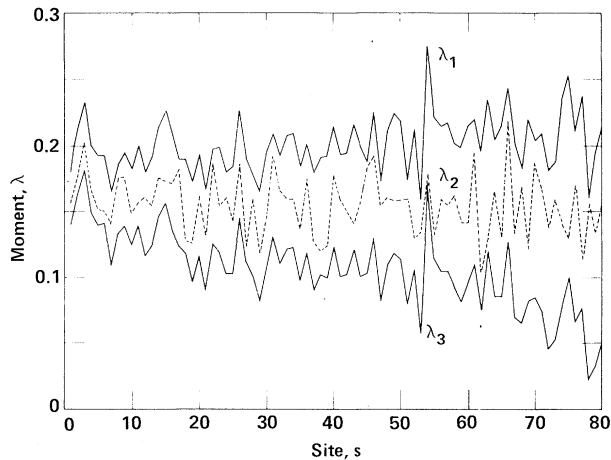


FIG. 3. Diagonal moments λ_i (see text) of the F ligand distribution about a Eu^{3+} ion in BeF_2 glass as a function of configuration. The sites are ordered with 7F_0 energy decreasing monotonically to the right.

the moments with energy, we plot λ_i as a function of Eu site in Fig. 3 for a subset of 80 configurations. The sites are ordered such that the 7F_0 energy decreases monotonically to the right. (The order of the sites was not found to be related to the order in which the initial fluid configurations were generated.) As the 7F_0 energy decreases (and the 5D_0 - 7F_0 separation increases), the average of λ_1 tends to increase slightly from ≈ 0.18 to ≈ 0.21 , λ_2 fluctuates randomly about ≈ 0.155 , and λ_3 decreases from ≈ 0.14 to ≈ 0.05 . The fluctuations in λ_1 and λ_3 are almost perfectly correlated with each other, while λ_2 exhibits less correlation, especially for the lower 7F_0 energies. From second-order perturbation theory, the energy of 7F_0 is

$$E({}^7F_0) \approx -\text{const}[(\lambda_1 - \lambda_2)^2 + (\lambda_1 - \lambda_3)^2 + (\lambda_2 - \lambda_3)^2]. \quad (2)$$

Because the variation of λ_3 is the largest, it is the most significant site parameter affecting the variation of $E({}^7F_0)$. Thus as the 7F_0 energy becomes more negative (and the 7F_1 splitting in-

creases), the ligand distribution about the RE tends to be more planar (λ_3 becomes small); for small splittings the moment distribution is more spherically symmetric (all λ_i nearly equal).¹² We have determined that there is no correlation between 7F_0 energy and coordination number. Therefore it is the symmetry of the ligand distribution that is responsible for the average behavior of the energy levels.

Finally we note that we have simulated glasses under several different quenching conditions and there are only small changes in the properties discussed here.

This work was supported by the U. S. Department of Energy Office of Basic Energy Sciences and by the Lawrence Livermore National Laboratory under Contract No. W-7405-Eng-48.

¹J. Wong and C. A. Angell, *Glass: Structure by Spectroscopy* (Dekker, New York, 1976).

²See, for example, C. Brecher and L. A. Riseberg, *Phys. Rev. B* **13**, 81 (1976).

³J. P. Hansen, *Phys. Rev. A* **8**, 3096 (1973).

⁴L. V. Woodcock, C. A. Angell, and P. Cheeseman, *J. Chem. Phys.* **65**, 1565 (1976); C. A. Angell, private communication.

⁵L. Pauling, *The Nature of the Chemical Bond* (Cornell Univ. Press, Ithaca, 1960).

⁶S. Brawer, to be published.

⁷J. Zarzycki, *Phys. Chem. Glasses* **12**, 97 (1971).

⁸A. J. Leadbetter and A. C. Wright, *J. Non-Cryst. Solids* **7**, 156 (1972).

⁹A. Rahman, R. H. Fowler, and A. H. Narten, *J. Chem. Phys.* **57**, 3010 (1972).

¹⁰This is a reasonable approximation because the sum $\sum_L q_L R_L^{-3}$ over ligands within 2.75 Å is (70–80)% of the sum $\sum_L q_L R_L^{-3}$ over all ions of the system. In addition, the closer ligands are expected to be proportionately more important because of wave-function-overlap contributions to the CF.

¹¹To match the wavelength of the transition in a fluoride glass, Rhodamine 6G was dissolved in trifluoroethylene. We thank Peter Hammond for recommending this combination.

¹²This does not, however, imply spherical symmetry at the site.